

# Application of bench-scale biocalorimetry to photoautotrophic cultures

Marcel Janssen<sup>a,\*</sup>, Rodrigo Patiño<sup>b</sup>, Urs von Stockar<sup>a</sup>

<sup>a</sup> Ecole Polytechnique Fédérale de Lausanne, Faculté des Sciences de Base, Institut des Sciences et Ingénierie Chimiques, Laboratoire de Génie Chimique et Biologique, Bâtiment CH-H, CH-1015 Lausanne, Switzerland

<sup>b</sup> Cinvestav Unidad Mérida, Departamento de Física Aplicada, Km. 6 Antigua Carretera a Progreso, AP 73 Cordomex C-P-97310, Mérida, Yucatán, Mexico

Received 1 November 2004; received in revised form 23 March 2005; accepted 2 April 2005

Available online 4 June 2005

## Abstract

Bench-scale biocalorimetry ( $\geq 1$  L) allows for the determination of the metabolic heat flow during bioprocesses under complete control of all process conditions for extended periods of time. It can be combined with a number of on-line and off-line measurement techniques. This combination can significantly improve insight into the metabolism of microorganisms and the optimization of bioprocesses. In this study it is demonstrated that bench-scale biocalorimetry can also be applied to phototrophic microorganisms. The green microalga *Chlorella vulgaris* CCAP 211/11B was cultivated in a Mettler-Toledo RC1 calorimeter adapted for high-sensitivity biological calorimetry (BioRC1). Heat production was monitored in 1.5 L batch cultures. In the linear phase of growth, inhibitors of photosynthetic electron transport (DCMU, 3-(3,4-dichlorophenyl)-1,1-dimethylurea, and DBMIB, 2,5-dibromo-3-methyl-6-isopropyl-*p*-benzoquinone), were used to stop photosynthesis and to monitor the resulting increase in the energy dissipating heat flux. This resulted in a calculated storage of light energy as chemical energy, i.e. biomass, of  $141 \pm 12.2 \text{ mW L}^{-1}$  ( $\pm$ S.D.). In addition, it was demonstrated that calorimetric determination of the total amount of light energy absorbed within the reactor was accurate by comparing two different calorimetric techniques. Using both the value of the total light input and the quantity stored as chemical energy, the photosynthetic efficiency could be calculated as 10.5% in this example.

© 2005 Elsevier B.V. All rights reserved.

**Keywords:** Biocalorimetry; Photosynthesis; Microalgae; Photosynthetic efficiency; *Chlorella*

## 1. Introduction

Although many microbiological processes have been studied with mL-scale [1] and bench-scale calorimetric techniques [2,3], only a limited number of papers describe the potential application of mL-scale calorimetry for the study of phototrophic processes [4–6]. In 1939, an mL-scale calorimetric method was used by Magee and coworkers to measure the quantum yield of photosynthesis in order to end a scientific debate on this issue [4]. In a 2.9 mL cuvette, microalgal cells (*Chlorella*) were illuminated at varying light intensities while measuring the heat consumption and production in experiments of less than an hour. A quantum yield of 0.077 was

determined which means that it takes 13 photons to reduce one molecule of carbon dioxide to the level of glucose. These results fit well with currently available data and the accepted Z-scheme of photosynthesis [7–9].

Decades later, this first successful application was followed by the application of mL-scale calorimetry for the study of the microalga *Chlorella* by Petrov and coworkers [5] and also for the study of spinach leaf by Johansson and Wadsö [6]. As compared to mL-scale calorimetry, bench-scale calorimetry ( $\geq 1$  L) allows for complete control of all relevant process conditions for extended periods of time, as for example chemostat cultures [10]. Moreover, on a bench-scale, biocalorimetry can be combined with a number of on-line and off-line measurement techniques within the same experiment. This combination of monitoring techniques significantly improves the insight into metabolism

\* Corresponding author. Tel.: +41 21 6933695; fax: +41 21 6933680.  
E-mail address: [marcel.janssen@epfl.ch](mailto:marcel.janssen@epfl.ch) (M. Janssen).

and adaptations of microorganisms under different conditions, possibly resembling those eventually used for industrial bioprocesses [11–13]. This study shows that bench-scale photobiocalorimetry is a feasible option for future work.

One might also use an mL-scale calorimeter as a flow-through cell connected to a fully controlled and monitored bench-scale photobioreactor. The efficiency of light utilization, however, and as a result metabolism, is strongly dependent on the light regime. Changes in the light regime influence extremely fast the efficiency of photobiological light utilization, within microseconds up to only a few seconds [14,15]. Results from measurements on the utilization of light energy in an mL-scale calorimeter therefore cannot be extrapolated to the level of the whole bioreactor. It is not possible to create the same light regime within the mL-scale calorimeter and its sample lines, as the algae experience within the bioreactor. This, and problems associated with wall-growth in the sample lines during long-term experiments, necessitates the application of calorimetry on the bench-scale photobioreactor itself.

Photobiocalorimetry is seriously hindered by the fact that the major part of the light energy absorbed by the microalgae is eventually dissipated as heat and only a small fraction is stored within new biomass, maximally 27% based on visible light [16]. In addition, the volumetric productivity of phototrophic processes in standard stirred-tank bioreactors is low, maximally  $2.5 \text{ mmol L}^{-1} \text{ h}^{-1}$  of biomass carbon but usually less [17,18]. For these reasons, a bench-scale calorimeter with a very small detection limit is needed. The successful application of an adapted Mettler-Toledo RC1 calorimeter (BioRC1) for measurements on weakly exothermic cultures [19–21] therefore also opened up the possibility for bench-scale photobiocalorimetry.

This study demonstrates that biocalorimetry can be applied on a bench-scale providing quantitative information on the storage of light energy during photoautotrophic cultivation of microalgae. The Mettler-Toledo RC1 reactor used was not developed for phototrophic cultures (low surface to volume ratio) and the productivity of photoautotrophic growth is severely limited by the surface which can be exposed to light. For this reason the experiments described here were based on a calorimetric ‘snap-shot’ during the linear growth phase of microalgal batch cultures. Consequently, the experiments were not hindered by long-term baseline drifts.

In the linear growth phase, photosynthesis was stopped by addition of two inhibitors of photosynthetic electron transport. The increase in heat flux measured was used to calculate the amount of light energy stored as chemical energy (biomass). In addition, it was demonstrated that calorimetric determination of the total amount of light energy absorbed within the bioreactor was accurate by comparing two different calorimetric techniques. Using both the value of the total light input and the amount stored as chemical energy, the photosynthetic efficiency could be calculated.

## 2. Materials and methods

### 2.1. Organism and medium

The green microalga *Chlorella vulgaris* CCAP 211/11B was derived from the Culture Collection of Algae and Protozoa (CCAP, Oban, Scotland). The cultivation medium was based on the one described by Mandalam and Pals-son [22] and was composed of (in  $\text{mmol L}^{-1}$ ):  $\text{KNO}_3$ , 29.7;  $\text{KH}_2\text{PO}_4$ , 5.44;  $\text{Na}_2\text{HPO}_4 \cdot 2\text{H}_2\text{O}$ , 1.46;  $\text{MgSO}_4 \cdot 7\text{H}_2\text{O}$ , 1.62;  $\text{CaCl}_2 \cdot 2\text{H}_2\text{O}$ , 0.088. In addition, the following (trace) elements were added (in  $\mu\text{mol L}^{-1}$ ):  $\text{FeSO}_4 \cdot 7\text{H}_2\text{O}$ , 316;  $\text{Na}_2\text{EDTA} \cdot 2\text{H}_2\text{O}$ , 316;  $\text{H}_3\text{BO}_3$ , 1.00;  $\text{MnCl}_2 \cdot 4\text{H}_2\text{O}$ , 65.6;  $\text{ZnSO}_4 \cdot 7\text{H}_2\text{O}$ , 11.1;  $\text{CuSO}_4 \cdot 5\text{H}_2\text{O}$ , 7.33. The pH was set to 6.7 with 4N NaOH.

*C. vulgaris* was maintained as 100 mL liquid cultures in 250 mL glass Erlenmeyer flasks closed with a cotton stoppers. Every 2 weeks cultures were transferred to new flasks with freshly prepared medium. The flasks were placed under mild fluorescent light at room temperature on an orbital shaker (100 rpm) and they were illuminated 24 h per day.

### 2.2. Photobiocalorimeter and illumination

A modified 2L commercial reaction calorimeter, RC1 from Mettler-Toledo AG (Switzerland) was used, the BioRC1. The software and hardware of this calorimeter were modified to increase the resolution as described elsewhere [19,20]. In addition, some of the modifications presented and tested by García-Payo and coworkers [21] were also applied (Fig. 1): (1) the head plate temperature was maintained at  $T_r + 2^\circ\text{C}$ ; (2) the reactor was placed in an insulating box; (3) a thermostatic circuit inside the box was maintained at  $T_r$  preventing large temperature fluctuations; (4) the modified version of the standard glass RC1 reactor was used.

As can be seen in Fig. 1 the reactor temperature ( $T_r$ ) was continuously monitored and maintained at

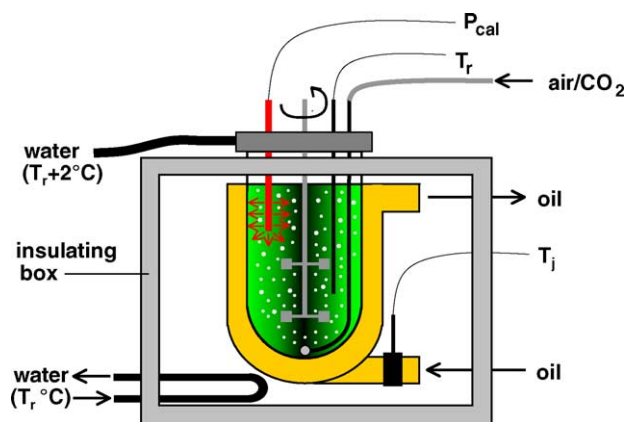


Fig. 1. Schematic presentation of the BioRC1 calorimeter hanging inside a closed insulating box (5 cm thick plexiglass wall).  $P_{\text{cal}}$  power calibration heater;  $T_r$  and  $T_j$  temperature of culture suspension and cooling/heating oil, respectively, both measured continuously with a PT100 probe. The culture is continuously gassed with an air/ $\text{CO}_2$  mixture. See text for more details.

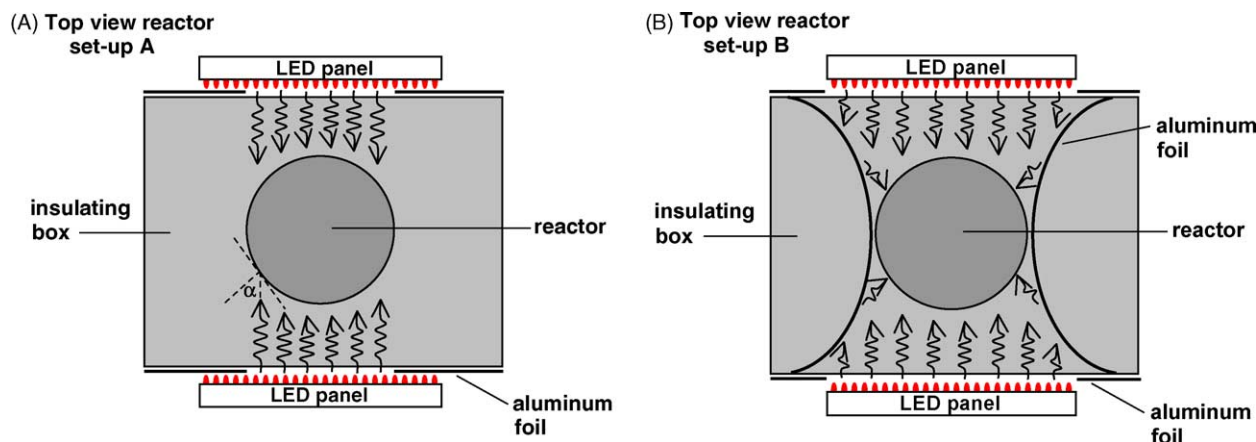


Fig. 2. Schematic presentation of the illumination of the culture grown in the BioRC1 calorimeter. A top view of the bioreactor set-up is presented. The lamps, two panels of red light emitting diodes, were positioned outside the insulating box. Two set-ups were used in this study: A and B. Set-up B provides for more light introduced in the bioreactor. See text for more details.

$25.0000 \pm 0.0005$  °C by adapting the oil temperature in the cooling jacket ( $T_j$ ) until a steady-state is reached, i.e. heat-conduction calorimetry. In this situation the temperature gradient between the culture suspension and cooling jacket is such that the rate of heat transfer exactly matches the rate of heat generation. This temperature gradient is continuously adapted by the BioRC1 control circuit as a response to changes in heat production rate. Using the calibration heater, the heat transfer coefficient of the cooling jacket can be determined and this coefficient is used to quantify the heat rate (power,  $P$ ) during the actual biological processes.

Mixing in the bioreactor was provided by two six-blade disc turbines connected to the central stirrer shaft. In addition, the reactor was gassed with an air/carbon dioxide mixture to provide carbon dioxide and to remove oxygen. The gas was humidified and heated before entering the biocalorimeter to limit the influence of evaporation and gas temperature fluctuations on the stability of the heat rate baseline. After passing through a  $0.2 \mu\text{m}$  filter, the gas was dispersed as very fine bubbles at the bottom of a 2 L DURAN bottle (Schott, Germany) filled with 2 L of water maintained at  $50 \pm 0.1$  °C. After this, the gas was led through a similar bottle maintained at  $T_r \pm 0.1$  °C before it was released in the reactor.

Light energy was supplied via two panels (width  $\times$  height = 20 cm  $\times$  30 cm) of 1452 light emitting diodes (LEDs) (Fig. 2). The LED type used was a Kingbright L-53SRC-F (Kingbright, UK) and its emission spectrum is shown in Fig. 3. The radiation emitted by the LED completely falls within the absorption range of chlorophyll-rich green microalgae and is suitable for the cultivation of *Chlorella* [23]. Above all, water and glass hardly absorb radiation with a wavelength lower than 700 nm.

The LED panels were positioned outside the insulating box. Using aluminum foil, all the light coming from the peripheral LEDs not directly focused onto the bioreactor was prevented from entering the box (Fig. 2, A). In set-up B,

less LEDs were shielded and more light was allowed to enter the box, which was re-directed into the bioreactor using aluminum foil mirrors fixed inside the box (Fig. 2, B). In set-up B, the baffles of the reactor were also removed to prevent light absorption by these parts. Ventilators were used to cool the panels, limiting the rate of decrease of LED output.

The reactor was further equipped with a pH and a Clark-type dissolved oxygen (DO) probe to monitor both variables continuously. The pH was controlled at 6.7 by the automatic addition of a nitric acid solution (150 mM). The gas supply was controlled with two mass flow controllers (Brooks Instruments BV, The Netherlands), one for air at  $400 \text{ mL min}^{-1}$  and one for carbon dioxide at  $12 \text{ mL min}^{-1}$  (3% v/v).

### 2.3. Experimental procedure

Two characteristic batch experiments will be presented and discussed. First, the reactor was filled with demineralized water and autoclaved in situ ( $121$  °C) with all

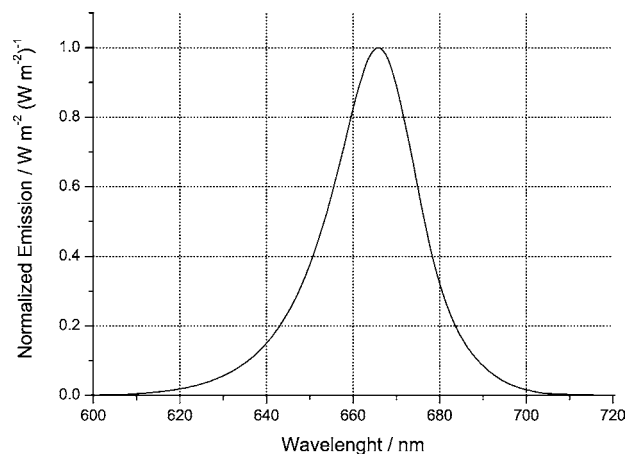


Fig. 3. Emission spectrum of Kingbright L-53SRC-F light emitting diodes (LEDs).

probes in place. The humidifying bottles, tubing and filters used for the gas supply were autoclaved separately at 121 °C. In addition, the nitric acid solution, all reactor connections, tubing for sampling, medium or acid addition, and the gas outlet were autoclaved separately and connected to the BioRC1 just after it cooled down. After this, the gas flow was started and the water was slowly released via a drain at the bottom of the reactor.

*C. vulgaris* cultures were pre-grown under red LED light in 250 mL Erlenmeyer flasks containing 100 mL medium as described before. After a week of acclimation one flask was used to inoculate 1.4 L filter-sterilized (0.22 µm) medium. The resulting 1.5 L was transferred to the bioreactor. When the reactor was filled with the medium containing the algae the BioRC1 was started in the isothermal ( $T_r$ ) mode at 25 °C and stirring was set at 200 rpm.

As mentioned before the reactor was gassed with air supplemented with 3%, v/v CO<sub>2</sub>. This led to a pH decrease due to the dissolution of CO<sub>2</sub>. In situ, the pH was therefore corrected to 6.7 in several steps by injecting 4N NaOH via a reactor port with septum. At this stage the LED lamps were still off. The calorimeter baseline was allowed to stabilize first and then a heat calibration was performed: the calibration heater was turned on for 45 min in the  $T_r$  mode of operation. Finally, 4–5 h after the addition of the medium with algae, the lights were turned on allowing the algae to grow.

The experiments were ended in the linear phase of growth when photosynthesis was stopped with two different inhibitors, DCMU (3-(3,4-dichlorophenyl)-1,1-dimethylurea) was used at 20 µM to stop the linear electron transport at photosystem II and DBMIB (2,5-dibromo-3-methyl-6-isopropyl-*p*-benzoquinone) was used at 2 µM to inhibit cyclic electron transport around photosystem I (personal communication Laurent Cournac, CEA Cadarache, France). DCMU was injected dissolved in 0.5 mL of ethanol and DBMIB in 0.5 mL of chloroform.

## 2.4. Analyses

### 2.4.1. Sampling

Samples were directly pumped out of the reactor with an automated system via an immersed sampling tube. Immediately after sampling, the remaining liquid in the lines was flushed back to the reactor with filtered (0.2 µm) air. The samples were stored at a temperature of 1 °C for 0 to 12 h depending on the time of sampling.

### 2.4.2. Optical density

The optical density was measured at 560 and 680 nm on an UVIKON 930 spectrophotometer (Kontron Instruments). If needed, samples were diluted with fresh medium.

### 2.4.3. Dry weight (*dw*)

Samples of 5–10 mL, containing several milligrams of dry biomass, were filtered over 0.2 µm Tuffryn® membrane filters (Gellman Sciences, Pall Corporation, USA) with an SM

16249 filtration unit (Sartorius, Germany). The filters were dried previously in a microwave (10 min, 150 W), allowed to cool down in a dessicator and weighed ( $W_1$ ). After sample filtration the filters were dried until constant weight ( $W_2$ ). The difference between  $W_2$  and  $W_1$  yielded the dry weight (*dw*).

### 2.4.4. Nitrate

Raw samples (1.5 mL) for nitrate analysis were first centrifuged in an Eppendorf tube (14 000 rpm, 10 min). The supernatant was filtered (0.2 µm), collected and stored at –18 °C until analysis. Nitrate in these samples was determined by an enzymatic bioassay (Cat. no. 10 905 658 035, Boehringer Mannheim/R-Biopharm, Germany) on a Cobas Mira chemistry system (Roche, Switzerland).

### 2.4.5. Off-gas analysis

The off-gas from the BioRC1 was analyzed for the volume fraction of oxygen (O<sub>2</sub>) and carbon dioxide (CO<sub>2</sub>). The gas from the BioRC1 was directly led through the analyzers. The oxygen fraction was measured with a Servomex (UK) series 1100 paramagnetic analyzer. Carbon dioxide was determined with a Servomex Xendos 2500 infrared analyzer.

## 3. Results and discussion

The experiment was performed at a light input of 0.88 W L<sup>-1</sup> (set-up A in Fig. 2). After reactor inoculation, starting the stirrer, opening the gas flow, and after stabilizing the pH, the biomass growth and the heat rate were monitored. The heat rate (power,  $P$ ) is presented in Fig. 4. After reaching a constant rate, a heat calibration was performed (event 1 in Fig. 4) to calculate the heat transfer coefficient, which was used to calculate the heat rate presented in this graph. After the heat calibration, the lights were turned on (event 2) and photoautotrophic growth could start. An immediate large increase in the heat rate due to the light energy absorbed and dissipated as heat can be seen. The biomass density was low ( $\pm 20$  mg dw L<sup>-1</sup>) and a considerable part of this heat must have been caused by light absorption by the reactor hardware (probes, sampling tube, stirrer, baffles and sparger).

From 20 h onwards the heat rate increases together with an increase in biomass density (Fig. 5). The multiplying cells intercept more and more of the light directed into the bioreactor. After 50 h, the power reaches a maximum (Fig. 4), from which time onwards all the light entering the reactor is absorbed within the reactor itself. In addition, the relative fraction of the light energy absorbed by the reactor hardware decreases. This non-biological light absorption is neglected because there were no means to determine this quantity and visual observation showed that the probes and stirrer were barely visible. Only a part of the baffles was clearly visible and this was the reason they were removed in the second experiment (B).

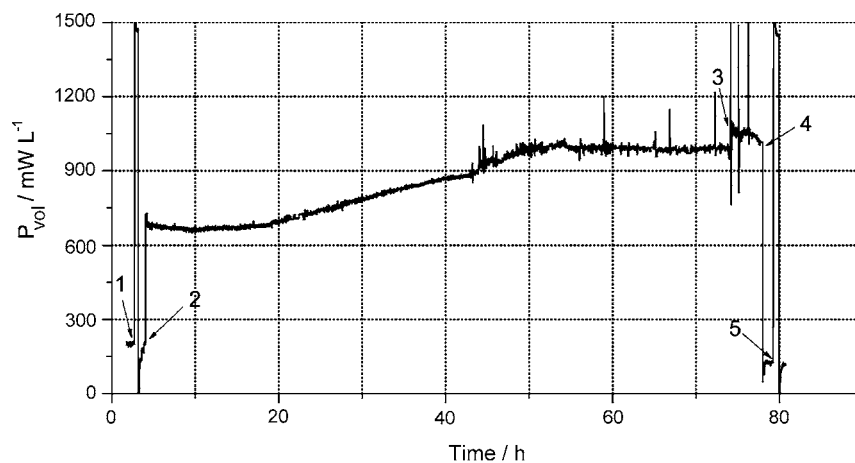


Fig. 4. Volumetric heat production rate (power,  $P_{vol}$ ) during batch cultivation of *C. vulgaris* in BioRC1 calorimeter. Light energy was provided according to set-up A (Fig. 2):  $0.88 \text{ WL}^{-1}$ . Events: (1) heat calibration; (2) lights on; (3) addition DCMU and DBMIB; (4) lights off; (5) heat calibration.

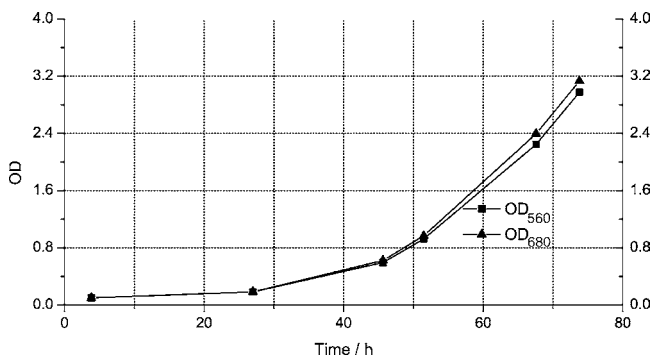


Fig. 5. Biomass growth measured as the optical density (OD) at 560 and 680 nm during batch cultivation of *C. vulgaris*. See Fig. 4 for more details.

The maximum power was constant (Fig. 4). In this stage, the absorption of light energy was constant and the microalgae were in the linear growth phase. The constant rate of supply of the limiting substrate, light, dictated a constant rate of increase in biomass density [24]. This can be seen in Fig. 5 and is confirmed with the dissolved oxygen (DO) concentration presented in Fig. 6. First the DO increased, reflecting an increase of the volumetric photosynthetic activity, until it

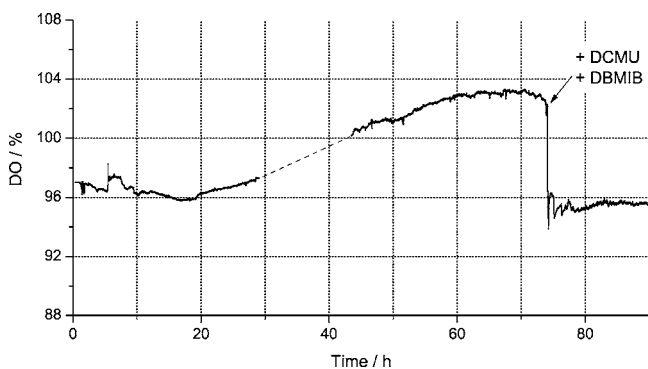


Fig. 6. Dissolved oxygen concentration (DO) during cultivation of *C. vulgaris* (Fig. 4). 100% corresponds to air-saturated medium at  $25^\circ\text{C}$ . The dashed line represents a period when the data acquisition was not working.

reached a maximum after 60 h. During the following hours, the DO in the culture liquid remained constant.

When the photosynthetic electron transport was stopped with the inhibitors, the dissolved oxygen concentration immediately dropped to a level comparable to the level before the lights were turned on, reflecting a complete inhibition of photosynthesis (Fig. 6). The heat rate also immediately responded to the inhibitors addition (event 3 in Fig. 4). After an initial thermal disturbance due to the addition, the RC1 control quickly established a new steady-state characterized by a higher heat rate. Because all conditions remained constant (pH, stirring, gassing, room temperature) this increase in heat rate is directly related to photosynthesis and it represents the light energy which was stored as chemical energy (new biomass) prior to the addition.

The part of Fig. 4 involving the inhibition has been enlarged and is shown in Fig. 7. Sampling of the reactor, just like the actual addition of inhibitors, led to sharp fluctuations in the heat flux caused by back flushing of the sample line (events 1, 2, 3 and 4 in Fig. 7). For this reason, the reactor temperature ( $T_r$ , Fig. 7) was used as a measure to determine which volumetric heat rate ( $P_{vol}$ ) data could be used for the determination of the average values before and after inhibition: only the values corresponding to a  $T_r < 25.0005^\circ\text{C}$  and  $> 24.9995^\circ\text{C}$  were taken into account. Subtracting the average volumetric power after inhibition from the one obtained before resulted in a value of  $62.5 \text{ mW L}^{-1}$  ( $\Delta P_{vol}$  'A' in Fig. 7), which represents the rate of light energy storage in biomass. Based on the standard deviation of these average values (dotted lines in Fig. 7) a standard deviation of  $15.1 \text{ mW L}^{-1}$  is calculated for the rate of light storage.

A second addition of inhibitors did not result in any significant changes. The addition of respiratory inhibitors (event 4, Fig. 7), Antimycin A ( $4 \mu\text{M}$ ) and propyl gallate ( $1 \text{ mM}$ ), resulted in a decrease of the heat flux. This was caused by a combination of factors such as foaming and a pH drop after these additions. Apparently, the concentration of the respiratory inhibitors was too high, leading to cell lysis.

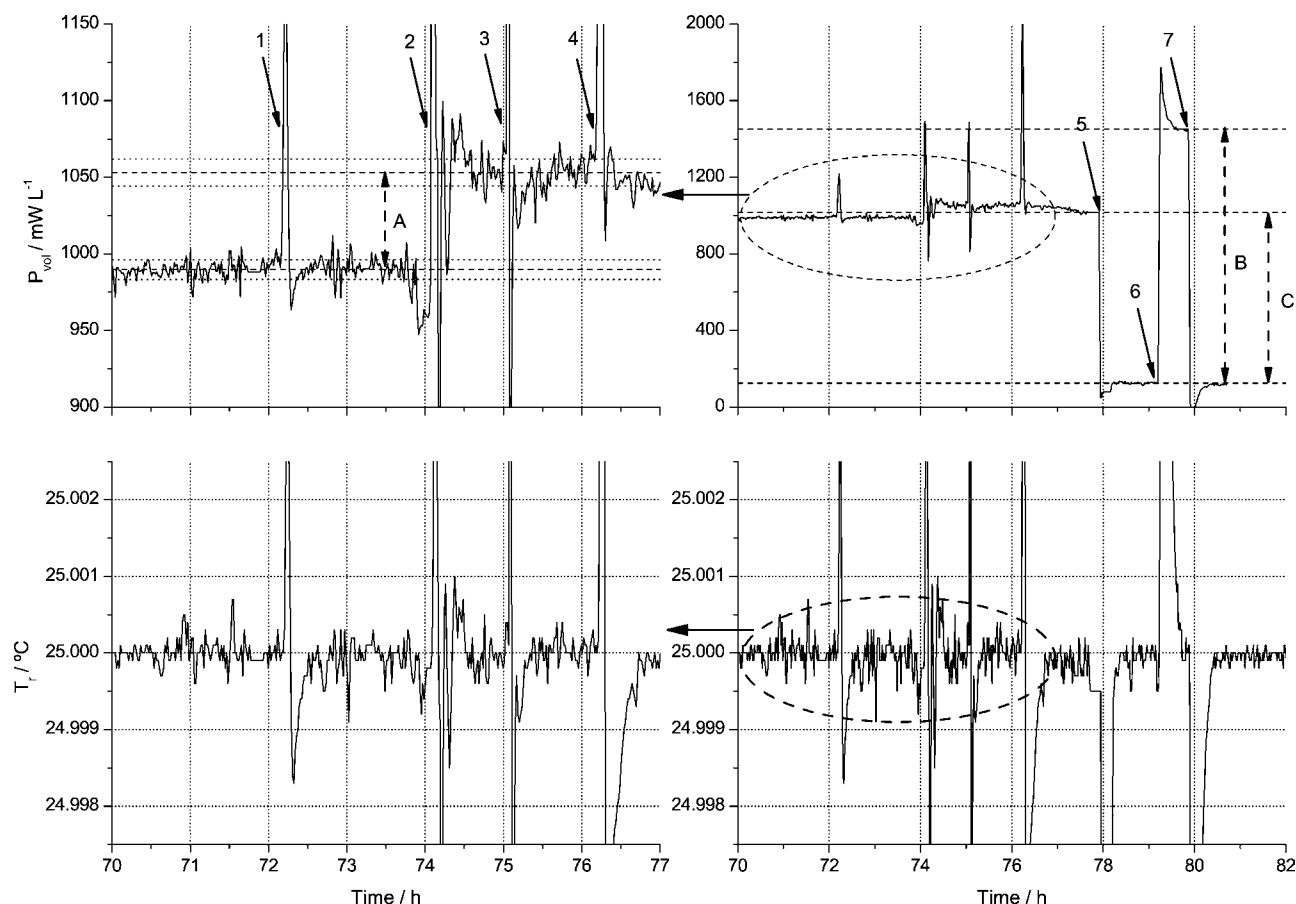


Fig. 7. Volumetric power ( $P_{\text{vol}}$ ) and reactor temperature ( $T_r$ ) at the time of photosynthesis inhibition during batch cultivation of *C. vulgaris* at a light input of  $0.88 \text{ WL}^{-1}$ . See Fig. 4 for more details. Events: (1) sampling; (2) addition of DCMU and DBMIB; (3) second addition of DCMU and DBMIB; (4) addition of respiratory inhibitors; (5) lights off; (6) calibration heater on and (7) off.  $\Delta P_{\text{vol}}$ : (A) photosynthesis-based consumption of light power; (B) calibrator power; (C) total light power. Dashed lines give average values of the volumetric heat rate ( $P_{\text{vol}}$ ) and dotted lines  $\pm$  the S.D. of  $P_{\text{vol}}$ .

At the moment the power stabilized, the lamps were turned off (event 5) and the decrease in volumetric heat rate observed represents the total rate of light energy absorption inside the bioreactor ( $\Delta P_{\text{vol}}$  'C', Fig. 7),  $0.88 \text{ WL}^{-1}$ . To verify the possible influence of changes in the room temperature or changes in liquid volume on the heat calibration, a second heat calibration was performed at the end (event 6–7 and  $\Delta P_{\text{vol}}$  'B', Fig. 7). The second heat calibration gave a calibration factor close to the first one ( $3.86$  as compared to  $3.97 \text{ WL}^{-1} \text{ K}^{-1}$ ) and was actually used for the calculations above.

Although it is demonstrated that the utilization of light energy can be quantified with biocalorimetry the accuracy is still low. The S.D. in the calculated photochemical light power consumption is  $15.1 \text{ mWL}^{-1}$  which is high as compared to the actually measured light power consumption of  $62.5 \text{ mWL}^{-1}$ . In a second experiment it was therefore attempted to increase the light input to reach a higher photosynthetic activity and, accordingly, a higher light power consumption. This was done using set-up B described in the Section 2 (see Fig. 2). More light of the LED panels was allowed to enter the insulated box and was re-directed into

the reactor using aluminum foil screens. In this way it was possible to increase the light input from  $0.88$  to  $1.35 \text{ WL}^{-1}$ .

Experiment B was performed under the same conditions as A and all the variables monitored showed the same characteristics as during experiment A. Again photosynthetic electron transport was inhibited in the linear phase of growth when the dissolved oxygen concentration had reached its maximum. This time the light power consumption, rate of light energy storage as chemical energy (biomass), was represented by a power of  $141 \pm 12.2 \text{ mWL}^{-1}$  ( $\Delta P_{\text{vol}}$  'A', Fig. 8). Consequently, the relative standard deviation of the measured light consumption is 9%. Although the accuracy of this first bench-scale test is not as good as that reached by mL-scale calorimetry [6], It already compares well with the accuracy of traditional methods to determine the yield of chemical energy (biomass) from light energy as explained below.

These traditional methods are based on separate measurement of both the light input to the bioreactor and the reactor productivity. The calibrations of commonly used photodiode-based light sensors are only guaranteed within a range of  $\pm 5\%$  from the measured value (LiCor, USA). These photo-

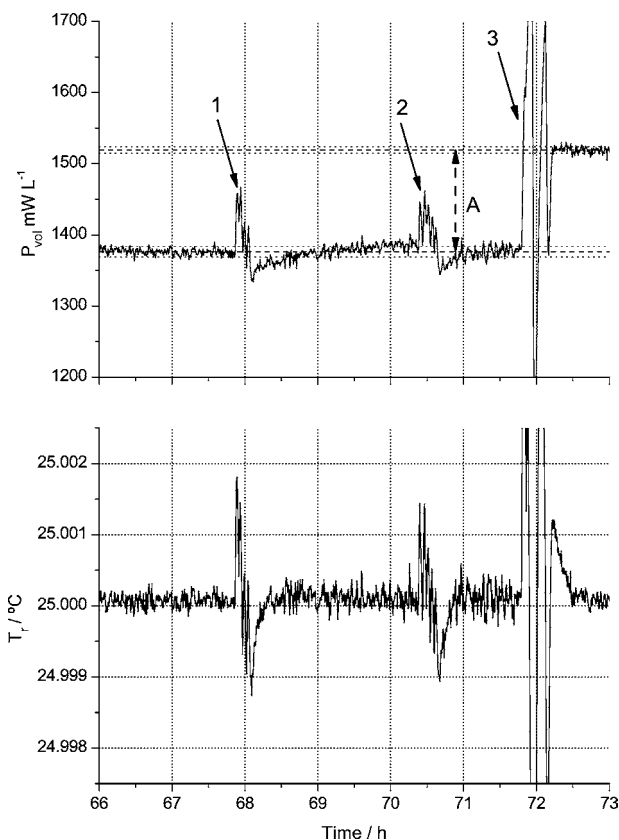


Fig. 8. Volumetric power ( $P_{\text{vol}}$ ) and reactor temperature ( $T_r$ ) at the time of photosynthesis inhibition during batch cultivation of *C. vulgaris* at a light input of  $1.35 \text{ W L}^{-1}$ , set-up B in Fig. 2. Events: (1) and (2) sampling; (3) addition of DCMU and DBMIB.  $\Delta P_{\text{vol}}$ : (A) photosynthesis-based consumption of light power. Dashed lines give average values of the volumetric heat rate ( $P_{\text{vol}}$ ) and dotted lines  $\pm$  the S.D. of  $P_{\text{vol}}$ .

diodes measure a light flux and, since this flux is inhomogeneous at the surface of a photobioreactor, the total light input is a variable with an error of 10% or more [25]. Secondly, the determination of the biomass productivity is based on sampling, measuring sample dry weight and determining the heat of combustion of the dry matter [26]. All these individual actions and measurements further increase the measurement error. For these reasons we can conclude that a relative standard deviation of 9% is not bad for a first test of bench-scale photobiocalorimetry.

In Table 1, the photosynthetic efficiency (PE) is presented together with other process variables. The PE represents the fraction of the total light input stored as chemical energy (biomass). In set-up A, the PE was found to be significantly lower than in set-up B. This might seem surprising because a higher light input usually is associated with a decrease in the photosynthetic efficiency. On the other hand, comparing set-up B to A (Fig. 2) it can be deduced that the extra light energy added to the reactor is added via the reactor walls that previously were hardly exposed to light. This could have lowered the average light flux at the reactor surface, which is beneficial for photosynthetic efficiency [27]. In addition,

Table 1

Summary of results from batch growth of *C. vulgaris* in BioRC1 calorimeter

	Set-up A: $0.88 \text{ W L}^{-1}$	Set-up B: $1.35 \text{ W L}^{-1}$
$\Delta_{\text{exp}}(\text{dw})$ ( $\text{g L}^{-1}$ )	0.50	0.64
$\Delta_{\text{exp}}(\text{NO}_3^-)$ ( $\text{mmol L}^{-1}$ )	4.2	6.8
$\Delta r_{\text{CO}_2}$ ( $\text{mmol L}^{-1} \text{ h}^{-1}$ )	0.51	1.2
$\Delta r_{\text{O}_2}$ ( $\text{mmol L}^{-1} \text{ h}^{-1}$ )	-0.81	-1.7
$\Delta \text{DO}$ (%)	-6.1	-9.5
PE (%)	7.1	10.5

$\Delta_{\text{exp}}(\text{dw})$ : dry weight production;  $\Delta_{\text{exp}}(\text{NO}_3^-)$ : nitrate consumption; PE: photosynthetic efficiency;  $\Delta r_{\text{CO}_2}$ ,  $\Delta r_{\text{O}_2}$  and  $\Delta \text{DO}$ : change in carbon dioxide and oxygen production rates, and change in dissolved oxygen (DO) concentration, respectively, following the inhibition of photosynthesis with DCMU and DBMIB. Production data are based on the off-gas analysis.

removing the baffles must also have increased the amount of light available to the microalgae.

The amount of nitrate consumed during the process corresponds with the biomass production, which was highest during experiment B (Table 1). It should be stressed that the highest PE does not necessarily have to correspond with the highest biomass concentration. In both experiments, batch growth was interrupted at an arbitrary moment in time at which the dissolved oxygen concentration (DO) was on its maximal level. More interesting therefore are the changes in oxygen production rate and carbon dioxide consumption rate upon inhibition, which are also presented in Table 1. Due to the low volumetric productivity the measurements are not very accurate; the overall change of the carbon dioxide and oxygen fraction in the off-gas is small in comparison to the resolution of 0.01% of the gas analyzers. Nevertheless all data support each other. Oxygen production and carbon dioxide consumption were significantly higher just before the interruption of experiment B in comparison to A. This all support the finding that the calorimetrically determined photobiological storage of light energy was significantly higher in set-up B than in A.

The inhibition of photosynthesis is assumed to be the only process leading to the power increase observed (Figs. 7 and 8). The baseline of volumetric heat rate, as determined during the first hours of the experiment (Fig. 4), is composed of heat terms related to stirring, evaporation and heat losses to the environment via the head plate and/or probes. The latter are dependent on the ambient temperature. All these processes do not change within the relatively short timeframe after inhibition of photosynthesis. Only a limited number of chemical and biological processes therefore could have influenced the observed shift of the heat rate.

Inhibition of photosynthesis halts  $\text{CO}_2$  consumption. Before inhibition, dissolution of carbon dioxide leads to a heat production of  $20.3 \text{ J mmol}^{-1} \text{ CO}_2$  [28]. The maximal consumption rate was estimated to be approximately  $1.0 \text{ mmol L}^{-1} \text{ h}^{-1}$ . An accurate quantification of this rate was not possible because of the large measurement error in the determination of  $\text{CO}_2$  consumption. Nevertheless, using this estimate, neglecting the dissolution of  $\text{CO}_2$  leads to an un-

derestimation of the photobiological light energy consumption of  $5.6 \text{ mW L}^{-1}$ .

The heat exchange involved with the addition of small quantities of solvent should also be considered. Together with the inhibitors DCMU and DBMIB, 0.5 mL of both ethanol and chloroform were added to the culture liquid. For this reason, an extra experiment was done under experimental conditions without biomass to determine the influence of these solvents on the heat rate. Half an hour after the addition of 0.5 mL ethanol and 0.5 mL of chloroform, a new thermal equilibrium was established and the power had decreased to  $7 \text{ mW L}^{-1}$ . A decrease in heat could be explained by evaporation of ethanol and/or chloroform. This would again imply that the photosynthesis related light consumption is underestimated.

Finally, the influence of respiratory activity on the determination of the storage of light energy should be discussed. Respiration is an integral part of the overall metabolism of microalgae under photoautotrophic conditions [29]. Many studies provide evidence that the respiration rate under photoautotrophic conditions is significantly higher than after dark incubation (>15 min) [30,31]. For the ideal overall determination of the efficiency of photoautotrophic growth both photosynthesis and respiration should be stopped at the end of the experiment. We were unable to stop respiration using specific inhibitors of mitochondrial electron transport because they induced cell lysis. This means that the photosynthesis related light consumption was overestimated by the magnitude of the unknown respiratory heat production rate after inhibition. On the other hand, in this experimental procedure a new steady-state was established. The constant power reached approximately 30 min after addition of the photosynthesis inhibitors indicates that the respiration did not change significantly. Apparently, respiration already approached the lower and constant respiration level usually seen after dark incubation.

### 3.1. Calorimetry as a tool to determine the light input in a photobioreactor

It was implicitly assumed that the determination of the light input ( $\Delta P_{\text{vol}} \text{ 'C'}$  in Fig. 7) was accurate. More specifically, it was assumed that the power decrease after turning off the lamps was completely caused by the sudden removal of absorption and dissipation of light energy by the microalgae. However, it is possible that light from the lamps misses the reactor and is absorbed by components of the insulating box. It is suspected that heating of the insulating box could influence the heat rate measured [21], in which case it would not reflect the true light absorption within the bioreactor. For this reason, the light input in set-up B was determined in two different ways. Both methods were done in the BioRC1 filled with 1.5 L of water made fully absorbing with 12.5 mL of black ink. To minimize other disturbing factors the reactor was not gassed and stirred at a rate of only 100 rpm.

According to the first method, i.e. heat-conduction calorimetry, the lights were turned on in the  $T_r$  mode of operation. Prior to this the heat transfer coefficient was calibrated with the calibration heater. According to the second temperature-rise method, the lights were turned on in the  $T_j$  mode of operation; the temperature of the cooling jacket ( $T_j$ ) remained constant and, consequently, only the reactor temperature ( $T_r$ ) increased and was closely monitored. After this, the calibration heater was used to induce a similar increase of  $T_r$ . The first method is the one used during the biological experiments and resulted in a light input of  $2.256 \text{ W}$  ( $1.492 \text{ W L}^{-1}$ ). The second method is a bit more complicated and will be discussed in detail below. The advantage of this method is the fact that the increase of  $T_r$  is not dependent on the temperature of the insulating box. The reactor contents are shielded from the insulating box by the cooling jacket (Fig. 1), which is maintained at a constant temperature,  $T_j$ .

The temperature increase of the reactor liquid during heating with the calibration heater can be described with:

$$c_{p,\text{med}} M_{\text{med}} \frac{dT_r}{dt} + c_{p,\text{ins}} M_{\text{ins}} \frac{dT_{\text{ins}}}{dt} = P_{\text{cal}} - UA(T_r - T_j),$$

$$\text{assuming } \frac{dT_{\text{ins}}}{dt} = \frac{dT_r}{dt}$$

this leads to:

$$(c_p M)_{\text{all}} \frac{dT_r}{dt} = P_{\text{cal}} - UA(T_r - T_j) \quad (1)$$

and therefore:

$$\ln(Y) = \frac{UA}{(c_p M)_{\text{all}}} t \quad (1a)$$

where:

$$Y = \left\{ \frac{q_{\text{cal}} - UA(T_{r,0} - T_j)}{q_{\text{cal}} - UA(T_{r,t} - T_j)} \right\}$$

where  $c_{p,\text{med}}$  is the heat capacity of the reactor medium ( $\text{J kg}^{-1} \text{ K}^{-1}$ ),  $M_{\text{med}}$  the mass of the medium (kg),  $c_{p,\text{ins}}$  the heat capacity of the reactor inserts ( $\text{J kg}^{-1} \text{ K}^{-1}$ ),  $M_{\text{ins}}$  the mass of the inserts (kg),  $T_{\text{ins}}$  the temperature of the inserts ( $^{\circ}\text{C}$ ),  $T_j$  the jacket temperature ( $^{\circ}\text{C}$ ),  $P_{\text{cal}}$  the power of the calibration heater (W),  $UA$  the calorimeter heat transfer coefficient ( $\text{W K}^{-1}$ ) and  $(c_p M)_{\text{all}}$  is the overall heat storage of the reactor ( $\text{J K}^{-1}$ ).

The temperature increase during actual illumination can be described as:

$$(c_p M)_{\text{all}} \frac{dT_r}{dt} = P_l - UA(T_r - T_j)$$

$$\text{With : } P_l = \text{light power(W)} \quad (2)$$

Working in a dynamic mode care has to be taken using the jacket temperature ( $T_j$ ) because of the appreciable heat capacity of the reactor wall. This was taken into account with a corrected jacket temperature (RC1 manual, Mettler-Toledo



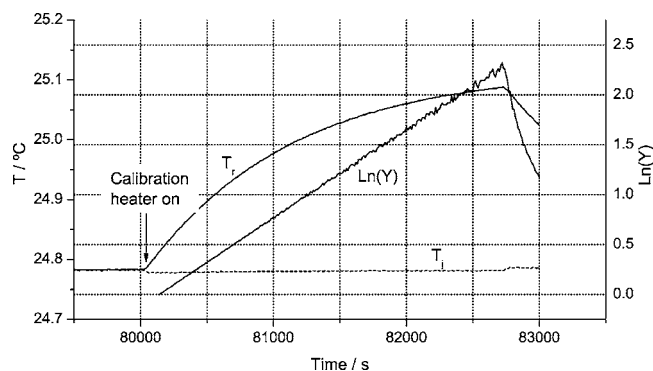


Fig. 9. Determination of heat capacity of the BioRC1 calorimeter by temperature-rise calorimetry.  $T_r$  and  $T_j$  represent reactor and jacket temperature, respectively. The variable  $Y$  is a function of  $T_r$  according to Eq. (1a). The BioRC1 was filled with 1.5 L de-mineralized water with 12.5 mL black ink.

AG, Switzerland). In Fig. 9 the increase of  $T_r$  is shown during heating with the calibration heater. Applying Eq. (1a) the overall heat capacity of the reactor ( $c_p M_{\text{all}}$ ) in  $\text{J K}^{-1}$ , can be calculated from the slope of the curve of  $\ln(Y)$  against time and the heat transfer coefficient ( $UA$ ). The heat transfer coefficient was already determined and, as a result, the overall heat capacity ( $c_p M_{\text{all}}$ ), was found to be  $6409 \text{ J K}^{-1}$ .

The heat capacity of the reactor can be entered in Eq. (2) and the increase of  $T_r$  with time after turning on the lights can be used to calculate the light power,  $P_I$  (Fig. 10). The variable  $P_I$  decreases from a higher initial value to a stable value, which is reached after 15 min. Apparently the LED output decreases, most likely due to heating of the lamps. The average light input after the initial 15 min was  $2.262 \text{ W}$  ( $1.496 \text{ W L}^{-1}$ ), almost equal to the value measured with heat-conduction calorimetry,  $2.256 \text{ W}$ . It is therefore concluded that the short-term effect of light-induced heating of the insulating box does not exist or can be neglected and that heat-conduction calorimetry is an accurate tool to measure the total light input.

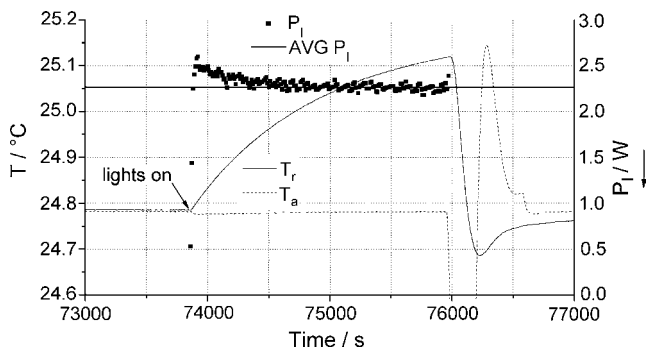


Fig. 10. Determination of the light energy input in the BioRC1 calorimeter by temperature-rise calorimetry. The square dots represent the light power,  $P_I$  in W, into the reactor determined for each 10 s interval according to Eq. (2). The horizontal line represents the average of these values between 75 000 and 76 000 s. See Fig. 9 for more details.

## 4. Conclusions

In this study it was demonstrated that the BioRC1 calorimeter could be adapted and applied for the calorimetric study of photoautotrophic growth. With the procedure developed it was shown to be possible to measure the amount of light energy stored as chemical energy during photoautotrophic growth. Moreover, it was demonstrated that the total amount of light energy absorbed could be accurately measured with calorimetry by two different methods. Consequently, combining both the value of the total light input and the amount stored as chemical energy the photosynthetic efficiency could be calculated. The photosynthetic efficiency during the linear growth phase of *Chlorella vulgaris* was 7.1% initially. An improvement in reactor illumination led to an improved efficiency of 10.5% stressing the importance of optimizing the light supply to reach higher productivity.

On-line monitoring of light utilization in phototrophic cultures during extended periods of time (several hours to days) should be the next step, exploiting the full potential of the non-invasive character of biocalorimetry. However, based on long-term baseline fluctuations [21], it is estimated that only in the situation the productivity, i.e. light storage, can be improved two-fold or more ( $\geq 300 \text{ mW L}^{-1}$ ) on-line monitoring becomes possible. Otherwise the detection limit is too high in comparison to the photosynthetic light consumption rate to be measured. Such an improvement in productivity agrees with the widely accepted view in microalgal biotechnology that the volumetric productivity of closed photobioreactors should be improved to yield an economically feasible exploitation of phototrophic microorganisms [32].

## References

- [1] I. Wadsö, Thermochim. Acta 394 (2002) 305–311.
- [2] T. Maskow, W. Babel, Thermochim. Acta 382 (2002) 229–237.
- [3] U. von Stockar, J.-S. Liu, Biochim. Biophys. Acta 1412 (1999) 191–211.
- [4] J.L. Magee, T.W. DeWitt, E. Coolidge Smith, F. Daniels, J. Am. Chem. Soc. 61 (1939) 3529–3533.
- [5] V.Y. Petrov, A.J. Alyabyev, N.L. Loseva, G.S. Klementyeva, V.I. Tribunskich, Thermochim. Acta 251 (1995) 351–356.
- [6] P. Johansson, I. Wadsö, J. Biochem. Biophys. Meth. 35 (1997) 103–114.
- [7] A.J. Walker, Trends Plants Sci. 7 (2002) 183–185.
- [8] J.H.A. Nugent, Eur. J. Biochem. 237 (1996) 519–531.
- [9] Govindjee, Photosynth. Res. 59 (1999) 249–254.
- [10] B. Birou, U. von Stockar, Enzyme Microb. Tech. 11 (1989) 12–16.
- [11] C. Herwig, I. Marison, U. von Stockar, Biotechnol. Bioeng. 75 (2001) 345–354.
- [12] C. Herwig, U. von Stockar, Bioproc. Biosyst. Eng. 24 (2002) 395–403.
- [13] P. Duboc, L.G. Cascao-Pereira, U. von Stockar, Biotechnol. Bioeng. 57 (1997) 610–619.
- [14] H.C.P. Matthijs, H. Balke, U.M. Hes van, B.M.A. Kroon, L.R. Mur, R.A. Binot, Biotechnol. Bioeng. 50 (1996) 98–107.
- [15] M. Janssen, M. de Winter, J. Tramper, L.R. Mur, J.F.H. Snel, R.H. Wijffels, J. Biotechnol. 78 (2000) 123–137.
- [16] R. Radmer, B. Kok, BioScience 27 (1977) 599–605.

- [17] H. Märkl, in: G. Shelef, C.J. Soeder (Eds.), *Algae Biomass*, Elsevier/North-Holland Biomedical Press, Amsterdam; New York, 1980, pp. 361–383.
- [18] E.M. Grima, J.M.F. Sevilla, J.A.S. Perez, F.G. Camacho, *J. Biotechnol.* 45 (1996) 59–69.
- [19] I. Marison, J.-S. Liu, S. Ampuero, U. von Stockar, B. Schenker, *Thermochim. Acta* 309 (1998) 157–173.
- [20] I. Marison, M. Linder, B. Schenker, *Thermochim. Acta* 310 (1998) 43–46.
- [21] M.C. García-Payo, S. Ampuero, J.-S. Liu, *Thermochim. Acta* 391 (2002) 25–39.
- [22] R.K. Mandalam, B.O. Palsson, *Biotechnol. Bioeng.* 59 (1998) 605–611.
- [23] C.G. Lee, B.O. Palsson, *Biotechnol. Prog.* 12 (1996) 249–256.
- [24] J.C. Ogbonna, H. Yada, H. Tanaka, *J. Ferment. Bioeng.* 80 (1995) 259–264.
- [25] A.S. Sánchez Mirón, E.M. Molina Grima, J.M.F. Fernández Sevilla, M.Y. Chisti, F.G. Garcia Camacho, *J. Appl. Phycol.* 12 (2000) 385–394.
- [26] G. Torzillo, P. Carlozzi, B. Pushparaj, E. Montaini, R. Materassi, *Biotechnol. Bioeng.* 42 (1993) 891–898.
- [27] J.C. Ogbonna, H. Yada, H. Tanaka, *J. Ferment. Bioeng.* 80 (1995) 369–376.
- [28] M. Meier-Schneiders, F. Schäfer, U. Grosshans, C. Busch, *Thermochim. Acta* 251 (1995) 85–97.
- [29] M.H.N. Hoefnagel, O.K. Atkin, J.T. Wiskich, *Biochim. Biophys. Acta* 1366 (1998) 235–255.
- [30] H.G. Weger, R. Herzig, P.G. Falkowski, D.H. Turpin, *Limnol. Oceanogr.* 7 (1989) 1153–1161.
- [31] X.P. Xue, D.A. Gauthier, D.H. Turpin, H.G. Weger, *Plant Physiol.* 112 (1996) 1005–1014.
- [32] M.R. Tredici, in: A. Richmond (Ed.), *Handbook of Microalgal Culture*, Blackwell Publishing, 2003, pp. 178–214.